Int. J. Heat Mass Transfer. Vol. 14, pp. 2157–2160. Pergamon Press 1971. Printed in Great Britain

ON THERMOCONVECTIVE INSTABILITY IN A BOUNDED CYLINDRICAL FLUID LAYER

G. S. CHARLSON and R. L. SANI
Department of Chemical Engineering, University of Illinois, Urbana, Illinois, U.S.A.

(*Received* 26 *January* 1971 *and in revised form* 22 *April* 1971)

NOMENCLATURE

A_{ijn},	coefficient in temperature field representation (2);
a,	wave number;
B_{ijn},	coefficient in velocity field representation (3);
D_{ijn},	coefficient in velocity field representation (3);
dv,	volume element;
$\boldsymbol{e}_r, \boldsymbol{e}_\phi, \boldsymbol{e}_z$,	unit vectors;
$G_n(\phi)$,	ϕ-trial function;
$J_n(r)$,	n-th order Bessel function of first kind;
K,	number of z-trial functions;
L,	number of r-trial functions;
M,	number of ϕ-trial functions;
Ra,	Rayleigh number;
$\boldsymbol{u}$,	dimensionless perturbation in velocity field;
V,	cylindrical domain;
w,	vertical component of dimensionless velocity;
X,	z-trial function;
Y,	r-trial function.

Greek symbols

α_k,	parameter in radial part of temperature trial function;
γ,	aspect ratio (radius-to-depth ratio);
ε,	"contained in";
θ,	dimensionless perturbation in temperature field;
λ,	inverse of square root of Rayleigh number;
ξ^4,	eigenvalue in (7);
ϕ,	azimuthal coordinate.

Special symbols

$\mho$,	linear vector space.

Superscripts

†,	transpose;
$'$,	derivative with respect to argument of function.

1. INTRODUCTION

IN AN earlier paper [1], the onset of axisymmetric convection in a cylindrical fluid layer heated from beneath was investigated for aspect ratios (radius-to-height ratios) from 1·0 to 8·0 and for selected larger aspect ratios. This communication extends that analysis to include the possibility of non-axisymmetric flows and hence completes the linear stability analysis of the system. In the interest of brevity the reader is referred to [1] for any pertinent nomenclature which is omitted here.

2. MATHEMATICAL DEVELOPMENT

It was shown in [1] that the mathematical characterization of the marginal stability state can be recast as a variational problem having the form

$$\lambda = \underset{(\boldsymbol{u},\theta)\,\varepsilon\mho}{\text{maximum}} \quad \frac{2\int \theta(\boldsymbol{e}_z\,.\,\boldsymbol{u})\,dv}{\int_v [\nabla\boldsymbol{u} : (\nabla\boldsymbol{u})^\dagger + \nabla\theta\,.\,\nabla\theta]\,dv}. \quad (1)$$

$\mho$ is a linear vector space of couples $(\boldsymbol{u}, \theta)$, each containing a solenoidal vector velocity field and an associated scalar temperature field, and each satisfying certain boundary constraints described in detail in [1].

In applying the Rayleigh–Ritz technique in the present case one can generalize the axisymmetric representations for u and θ used in [1] in the following manner:

$$\theta = \sum_{i=1}^{K}\sum_{j=1}^{L}\sum_{n=1}^{M} A_{ijn}\Phi_{ijn}(r, \phi, z); \quad (2)$$

$$\boldsymbol{u} = \sum_{i=1}^{K}\sum_{j=1}^{L}\sum_{n=1}^{M} B_{ijn}W_{ijn}(r, \phi, z) + D_{ijn}V_{ijn}(r, \phi, z). \quad (3)$$

The functions Φ_{ijn}, W_{ijn} and V_{ijn} are chosen to have the form:

$$\Phi_{ijn}(r, \phi, z) \equiv G_n(\phi)\,J_n(\alpha_j r)\sin(i\pi z); \quad (4)$$

$$W_{ijn}(r, \phi, z) \equiv G_n(\phi)\,[r^{-1}Y_{jn}(r)\,X_i'(z)\,\boldsymbol{e}_r - r^{-1}\,Y_{jn}'(r)\,X_i(z)\,\boldsymbol{e}_z]; \quad (5)$$

$$V_{ijn}(r, \phi, z) \equiv G_n(\phi)\,[-(\sqrt{-1})\,Y_{jn}(r)\,X_i'(z)\boldsymbol{e}_\phi + nr^{-2}\,Y_{jn}(r)\,X_i(z)\,\boldsymbol{e}_z]. \quad (6)$$

Here $Y_{jn}(r)$ are the eigenfunctions of the following eigenvalue problem:

$$\left[\frac{d^2}{dr^2} + \frac{1}{r}\frac{d}{dr} - \frac{(n+1)^2}{r^2}\right]^2 \left[r^{-1} Y_{jn}(r)\right] = \xi^4{}_{jn}\, Y_{jn}(r); \quad (7)$$

$$Y_{jn}(r) = Y'_{jn}(r) = 0, \quad r = 0 \text{ and } 1. \quad (8)$$

The functions $X_i(z)$ are defined as in [1] and

$$G_n(\phi) \equiv \left[\frac{1}{2\pi}\right]^{\frac{1}{2}} e^{-(\sqrt{-1})n\phi}. \quad (9)$$

Finally, the α's are roots of either

$$J_n(\alpha) = 0 \text{ (conducting lateral wall)} \quad (10)$$

or

$$\alpha J_{n-1}(\alpha) - nJ_n(\alpha) = 0 \text{ (insulating lateral wall)}. \quad (11)$$

It is noteworthy that each W_{ijn} and each V_{ijn} represents a solenoidal vector field and hence after Davis [2] could be referred to as a finite roll. The value of the index n characterizes the number of zero planes to be found in a rotation of ϕ through 360°; for example, the axisymmetric representations of [1] correspond to $n = 0$.

Substitution of these representations into (1) and application of the necessary conditions for a maximum lead to an algebraic eigenvalue problem for determining λ and the constants A_{ijn}, B_{ijn} and D_{ijn} to within a multiplicative factor.

A lower bound analysis identical in format to that performed in [1] can also be performed. In the case of non-axisymmetric flow states the counterpart of equation (39) of [1] is

$$w = C\,G_n(\phi)\,J_n(a\gamma r)\,F(z) \quad (12)$$

in which $F(z)$ is defined as in [1]. Here the permissible values of the parameter "a" are the roots of the transcendental equation

$$a\gamma J_{n+1}(a\gamma) + nJ_n(a\gamma) = 0. \quad (13)$$

The corresponding locus of lower bounds for a fixed value of n, i.e. azimuthal flow state, is *not* displayed here in Figs. (1)-(3) but Fig. 7 of [1] displays the characteristic behavior in all cases. The lower bound becomes increasingly sharp as the aspect ratio increases as expected since the lower bound is obtained by allowing slip on the lateral wall and represents an exact solution in the limit of infinite aspect ratio. Conversely, the lower bound is not extremely sharp for small aspect ratios. In the latter case a sharper lower bound can be obtained by satisfying the no-slip condition on the lateral wall but allowing slip on the top and bottom. The exact analysis of this case is available in the literature [3-6] and hence provides a convenient lower bound for small aspect ratios. The validity of such a lower bound can be established by obvious modifications of Sec. 5 in [1]. Such a combination of lower bounds has been *formally* applied by Catton and Edwards [11] to characterize the marginal stability state of the present system.

3. RESULTS AND DISCUSSION

The stability curves for axisymmetric and selected non-axisymmetric flow states are displayed in Fig. 1 for aspect ratios less than unity. It is noteworthy that there exists a transition in the marginal dynamic state from an axisymmetric state to an antisymmetric $n = 1$ state as the aspect ratio decreases. The transition point depends on the thermal condition imposed on the lateral wall, being approximately $\gamma = 0{\cdot}81$ for an insulating lateral wall and $\gamma = 0{\cdot}61$ for a conducting lateral wall. The occurrence of an antisymmetric dynamic state is in agreement with the experimental observations of Ostroumov [7] and others [8, 9]. The critical values of the Rayleigh number predicted in this case lie above those predicted originally by Hales [4] and subsequently extended by Verhoeven [3], Yih [5] and Catton and Edwards [6]; the disparity between the values presented herein and those of the latter authors decreases to zero as the aspect ratio approaches zero. This behavior is expected since, as established in Sec. 2, the results of Hale, Verhoeven, and Catton and Edwards represent sharp lower bounds for small values of the aspect ratio and an exact solution for the zero aspect ratio limit.

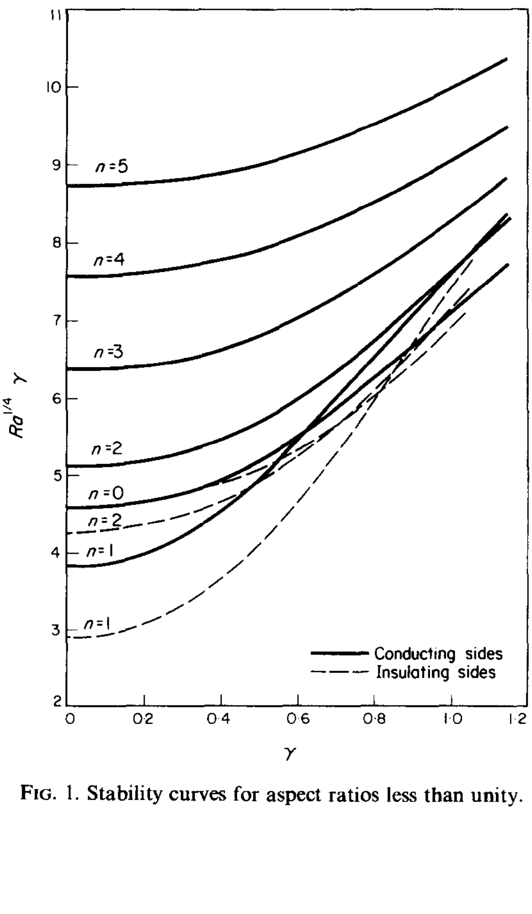

FIG. 1. Stability curves for aspect ratios less than unity.

The dependence of Rayleigh number on aspect ratio is displayed in Figs. 2 and 3 for aspect ratios greater than unity. There are three features worthy of comment. First, the convergence of the curves representing various n-states at large aspect ratios is to be expected if the characteristic cellular array of an infinite layer [10] is to be approximated by representations (2) and (3). Moreover, the validity of this behavior has previously been proven by Sani [11]. Second, the critical value of the Rayleigh number as obtained from either Fig. 2 or Fig. 3 by selecting the smallest value of Ra at each value of γ is within 10 per cent of the limiting infinite layer value of 1708 for aspect ratios greater than approximately 2. That is, when the radius is greater than twice the depth of the fluid layer the viscous dissipation at the lateral

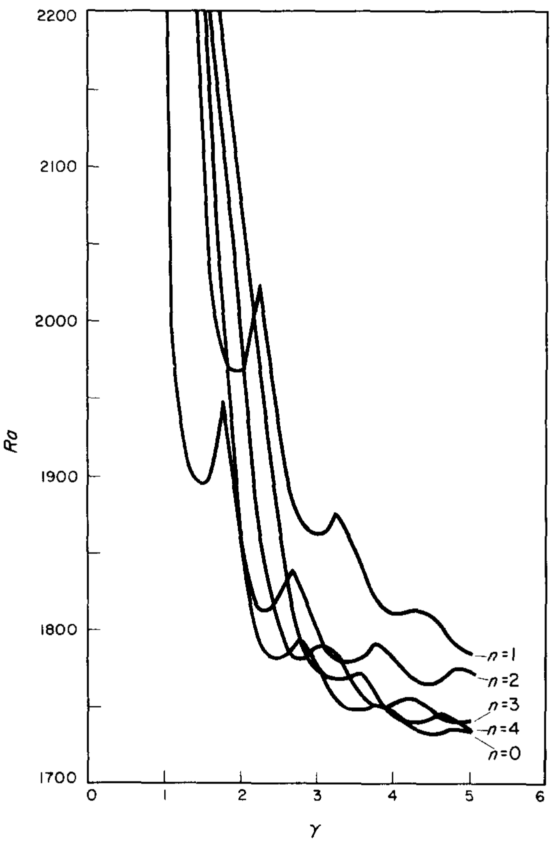

FIG. 2. Stability curves for insulating lateral wall and aspect ratios greater than unity.

wall plays a minor role in determining the energy requirements of the system. Third, nonaxisymmetric critical states are possible at least for various "patches" of aspect ratios when the aspect ratio is larger than approximately 2·8 in the case of an insulated lateral wall. These patches cover a

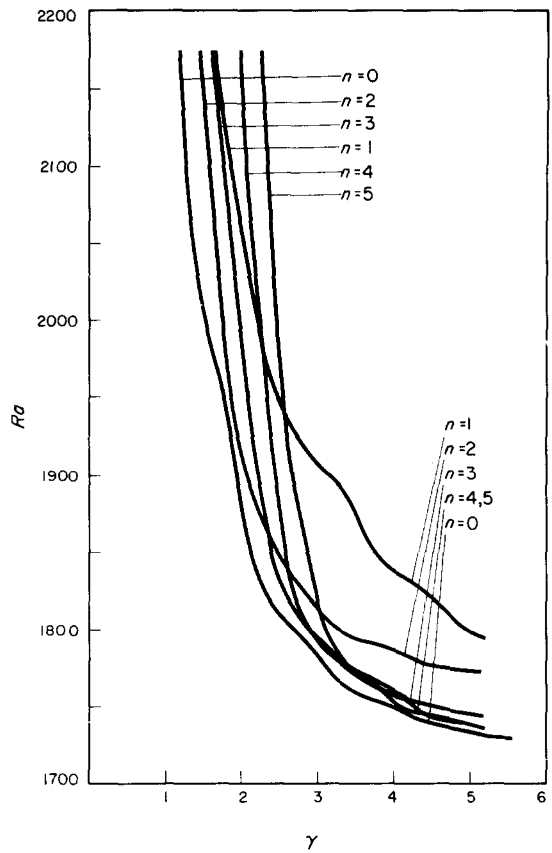

FIG. 3. Stability curves for conducting lateral wall and aspect ratios greater than unity.

neighborhood of the aspect ratio at which the number of radial cells changes in the axisymmetric case. As the number of possible n-states is increased more of these transition regions are effected. The same phenomenon may, or may not, occur in the case of a conducting lateral wall. The monotone decreasing nature of the stability curves (Fig. 3) may surpress the occurrence of these patches altogether or at least cause them to appear at larger aspect ratios. (The monotonicity can be established directly from the variational formulation and hence is *not* a ramification of any numerical procedures.) Preliminary numerical calculations suggest a complete suppression up to reasonably large aspect ratios but a difinitive answer probably cannot be based on numerical calculations due to the required accuracy. Thus, axisymmetric flow states, although observable at large aspect ratio [12–14], are a completely dominent structure, independent of the thermal condition imposed at the lateral wall, only in a narrow band of aspect ratios about unity.

The results presented herein coupled with those presented in [1] complete the linear stability analysis of the system as well as lead to some insight in interpreting some of the seemingly contradictory experiments reported in the literature. For example, Chen and Whitehead [15] induced stable straight rolls in a cylindrical container at slightly supercritical Rayleigh numbers while Koschmieder [11–13] observes axisymmetric rolls and Somerscales and Dougherty [16] first detect a hexagonal regime. All these experiments were performed at aspect ratios near, or greater than, ten. In order to reconcile these observations one must first recall that *all* the Rayleigh number versus aspect ratio curves for *all* n-states corresponding to a dynamic state with one cell in the vertical converge to 1708 as γ approached infinity. For example, as shown in [1] for the axisymmetric case ($n = 0$) the first three Rayleigh number values are already close at $\gamma = 10$. Moreover, the separation between these Rayleigh numbers is entirely due to the influence of the lateral wall whose effect decreases with increasing aspect ratio until the degenerate case of an infinite layer is reached where second order effects determine the cellular form. In addition according to the analysis the development of axisymmetric marginal flow states is dependent on adequate control of the thermal condition imposed at the lateral wall. That is, the manifestation of the so-called "wall effect" is not only dependent on the size of the fluid layer but also on the thermal state of the lateral wall. Consequently, at large aspect ratios the control of the experiment as well as the magnitude of secondary effects such as the temperature dependence of various physical parameters can play equal roles. Since various authors may use different fluids and control their experiments to varying degrees, it is not surprising that at large aspect ratios a myriad of cellular forms appear to have been observed. The analytical description of such cellular forms has recently been dealt with by Newell and Whitehead [17] and Segel [18] for infinite aspect ratios and "large" aspect ratios, respectively. The subtleties introduced by the small energy gap between dynamic states are exemplified in Segel's results which lead to a very good approximation to the critical Rayleigh number but predict a 2-*D* velocity field which, while being a good approximation, is not a possible solution of the linear stability problem [19, 20].

In closing it is noteworthy that in all cases the theory predicts a marginally stable dynamic state with one cell in the vertical. The latter is in agreement with all experimental observations known to the authors.

REFERENCES

1. G. S. Charlson and R. L. Sani, Thermoconvective instability in a bounded cylindrical fluid layer, *Int. J. Heat Mass Transfer* **13**, 1479–1496 (1970).
2. S. H. Davis, Convection in a box: linear theory, *J. Fluid Mech.* **30**, 465–478 (1967).
3. J. D. Verhoeven, Experimental study of thermal convection in a vertical cylinder of mercury heated from beneath, *Physics Fluids* **12**, 1733–1739 (1969).
4. A. L. Hales, Convective currents in geysers, *Mon. Not. R. Astr. Soc. Geophys. Suppl* **4**, 122–131 (1937).
5. C. S. Yih, Thermal instability of viscous fluids, *Q. Appl. Math.* **17**, 25–42 (1959).
6. I. Catton and D. K. Edwards, Initiation of thermal convection in finite right circular cylinders, *A.I.Ch.E. Jl* **16**, 594–601 (1970).
7. G. A. Ostroumov, *Svobodnaya convectzia v ousloviakh vnoutrennei zadachi*, State Publishing House, Technico-Theoretical Literature, Moscow–Leningrad (1952) (Eng. trans.: NACA-TM-1407 (1958)).
8. V. V. Slavnov, Free heat convection in metallic vertical tubes of circular section, *Soviet Phys. Tech. Phys.* **1**, 1938–1941 (1956).
9. E. I. Slavnova, The cellular structure of a convection flow in a vertical cylinder of round section, *Inzh.-fiz. Zh.* **4**, 80–86 (1961).
10. A. Pellew and R. V. Southwell, On maintained convective motion in a fluid heated from below, *Proc. R. Soc.* **176A**, 312–343 (1940).
11. R. L. Sani, Note on flow instability in heated ducts, *Z. Angew. Math. Phys.* **15**, 381–387 (1964).
12. E. Koschmieder, On convection on a uniformly heated plane, *Beitr. Phys. Atmos.* **39**, 1–11 (1966).
13. E. Koschmieder, On convection on a uniformly heated rotating plane, *Beitr. Phys. Atmos.* **40**, 216–225 (1967).
14. E. Koschmieder, On the wavelength of convective motions, *J. Fluid Mech.* **35**, 527–530 (1969).
15. M. M. Chen and J. A. Whitehead, Evaluation of two-dimensional periodic Rayleigh convection cells of arbitrary wave-numbers, *J. Fluid Mech.* **31**, 1015 (1968).
16. E. F. C. Somerscales and T. S. Dougherty, Observed flow patterns at the initiation of convection in a horizontal liquid layer heated from below, *J. Fluid Mech.* **42**, 755–768 (1970).
17. A. C. Newell and J. A. Whitehead, Finite bandwidth, finite amplitude convection, *J. Fluid Mech.* **38**, 279–303 (1969).
18. L. A. Segel, Distant side-walls cause slow amplitude modulation of cellular convection, *J. Fluid Mech.* **38**, 203–224 (1969).
19. R. P. Davies-Jones, Thermal convection in an infinite channel with no-slip sidewalls, *J. Fluid Mech.* **44**, 695–704 (1970).
20. P. Jennings, M. S. Thesis, Univ. Illinois, Urbana, Illinois (1971).